Available online at www.sciencedirect.com
ScienceDirect
Developmental Biology 307 (2007) 340–355
DEVELOPMENTAL BIOLOGY
www.elsevier.com/locate/ydbio

Identification and characterization of a novel Schwann and outflow tract endocardial cushion lineage-restricted *periostin* enhancer

Andrew Lindsley [a], Paige Snider [a], Hongming Zhou [a], Rhonda Rogers [a], Jian Wang [a], Michael Olaopa [a], Agnieszka Kruzynska-Frejtag [b], Shrinagesh V. Koushik [c,1], Brenda Lilly [c], John B.E. Burch [d], Anthony B. Firulli [a], Simon J. Conway [a,*]

[a] *Cardiovascular Development Group, Herman B Wells Center for Pediatric Research, Indiana University School of Medicine, Indianapolis, IN 46202, USA*
[b] *Wroclaw Medical University, 50-367 Wrocław, Poland*
[c] *Vascular Biology Center, Medical College of Georgia, Augusta, Georgia, GA 30912, USA*
[d] *Fox Chase Cancer Center, 333 Cottman Avenue, Philadelphia, PA 19111, USA*

Received for publication 12 December 2006; revised 17 April 2007; accepted 30 April 2007
Available online 3 May 2007

Abstract

Periostin is a *fasciclin*-containing adhesive glycoprotein that facilitates the migration and differentiation of cells that have undergone epithelial–mesenchymal transformation during embryogenesis and in pathological conditions. Despite the importance of post-transformational differentiation as a general developmental mechanism, little is known how *periostin*'s embryonic expression is regulated. To help resolve this deficiency, a 3.9-kb *periostin* proximal promoter was isolated and shown to drive tissue-specific expression in the neural crest-derived Schwann cell lineage and in a subpopulation of *periostin*-expressing cells in the cardiac outflow tract endocardial cushions. In order to identify the enhancer and associated DNA binding factor(s) responsible, *in vitro* promoter dissection was undertaken in a Schwannoma line. Ultimately a 304-bp^{peri} enhancer was identified and shown to be capable of recapitulating 3.9 kb$^{peri\text{-}lacZ}$ *in vivo* spatiotemporal patterns. Further mutational and EMSA analysis helped identify a minimal 37-bp region that is bound by the *YY1* transcription factor. The 37-bp enhancer was subsequently shown to be essential for *in vivo* 3.9 kb$^{peri\text{-}lacZ}$ promoter activity. Taken together, these studies identify an evolutionary-conserved *YY1*-binding 37-bp region within a 304-bp *periostin* core enhancer that is capable of regulating simultaneous novel tissue-specific *periostin* expression in the cardiac outflow-tract cushion mesenchyme and Schwann cell lineages.

Keywords: *Periostin*; Mouse embryo; Schwann cells; Heart development; Endocardial cushions; Peripheral nervous system; Lineage restricted promoter; *lacZ* reporter mice

Introduction

Periostin was originally isolated as osteoblast-specific factor-2 from the mouse osteoblastic cell line MC3T3-E1 (Takeshita et al., 1993). There are five human *periostin* isoforms, with variations occurring in the C-terminal domain constituting in-frame deletions or insertions, implying alternative splicing events (Litvin et al., 2004). The gene is structurally similar to *Fasciclin-I*, a *Drosophila* protein expressed in the peripheral nervous system (PNS) and specific central nervous system axonal bundles (McAllister et al., 1992). *Fasciclin-I* functions in guidance of migrating cells, cell sorting and adhesion during insect nervous system morphogenesis (Takeshita et al., 1993). The fasciclin extracellular domain is repeated four times in periostin and is evolutionary conserved from man to bacteria (Kawamoto et al., 1998). There are thought to be both membrane-associated forms and secreted forms (Litvin et al., 2005; Kudo et al., 2006). Interestingly, periostin can support osteoblast attachment and spreading.

* Corresponding author. Riley Hospital for Children, 1044 West Walnut Street, Room R4 W379, Indiana University School of Medicine, Indianapolis, IN 46202, USA. Fax: +1 317 2785413.
E-mail address: siconway@iupui.edu (S.J. Conway).
[1] Present Address: National Institute on Alcohol Abuse and Alcoholism, National Institutes of Health, Bethesda, MD 20892, USA.

0012-1606/$ - see front matter © 2007 Elsevier Inc. All rights reserved.
doi:10.1016/j.ydbio.2007.04.041

Moreover, periostin may be a ligand for $\alpha_v\beta_3$ and $\alpha_v\beta_5$ integrins and promote integrin-dependent cell adhesion and enhance cell motility (Gillan et al., 2002). Recently, periostin has been shown to preferentially localize in collagen-rich tissues and can directly interact with collagen Type-I fibrils (Norris et al. 2007). Periostin is widely expressed in normal embryonic/adult tissues and is highly expressed in diverse pathological conditions. Multiple reports have demonstrated elevated serum levels in tumor samples from neuroblastoma (Sasaki et al., 2002), elevated expression in head/neck carcinoma samples (Kudo et al., 2006; Gonzalez et al., 2003), as a novel component of subepithelial fibrosis in bronchial asthma (Takayama et al., 2006), in response to vascular injury (Li et al., 2005), in epithelial ovarian cancer (Gillan et al., 2002) and in patients with bone metastases from breast cancer (Sasaki et al., 2004) that had undergone epithelial–mesenchymal transformation (EMT) and metastasized. Significantly, periostin has been shown to potently promote post-EMT metastatic growth of colon cancer by augmenting cell survival via the Akt/PKB pathway (Bao et al., 2004). It is also thought to be responsible for extracellular matrix (ECM) deposition following myocardial infarction and pathological transformation (Stanton et al., 2000). In normal tissues, *periostin* is expressed during recruitment and attachment of osteoblast precursors in the fibrous periosteum (Horiuchi et al., 1999; Oshima et al., 2002; Litvin et al., 2004), post-EMT valve formation and remodeling (Kruzynska-Frejtag et al., 2001; Lindsley et al., 2005; Litvin et al., 2005), cranial suture maturation (Oshima et al., 2002) and during epithelial–mesenchymal signaling associated with craniofacial development (Kruzynska-Frejtag et al., 2004). We demonstrated via targeted deletion that *periostin* (*peri*^{lacZ}) null mice are predominantly viable and exhibit dwarfism, incisor enamel defects and an early-onset periodontal disease-like phenotype (Rios et al., 2005). Similarly, Kii et al. (2006) showed that *periostin is* required for eruption of incisors in mice. Combined, these mouse knockout data suggest that periostin may be required *in utero* for events that manifest themselves in postnatal life (Rios et al., 2005).

Despite the complex and intriguing correlation of disregulated *periostin* expression levels in both normal and pathological transformation conditions, very little is known about how *periostin* is transcriptionally controlled. Thus, unraveling the molecular mechanisms that regulate *periostin* expression could prove useful for gaining an understanding of numerous neoplastic diseases as well as normal bone, craniofacial and heart homeostasis. During osteoblast differentiation, transcription of *periostin* may be regulated by the bHLH transcription factor, *Twist* (Oshima et al., 2002), that is associated with EMT during tumor progression (Yang et al., 2004). To begin to clarify the molecular regulation of *periostin* gene expression, we used bioinformatics and cross-species comparisons to identify seven highly conserved regions within the proximal 3900 base pairs of the *periostin* promoter. We subsequently cloned the 5′ mouse 3.9-kb *periostin* promoter and *in vivo* transgenic reporter analysis revealed lineage-restricted *in utero* expression within only Schwann cells and in a subpopulation of endogenous periostin-expressing cardiac outflow tract (OFT) endocardial cushion cells. Using EMSA and serial truncation/internal deletion luciferase reporter *in vitro* assays, we demonstrate that a 37-bp enhancer is necessary and that the ubiquitous *Ying Yang-1* (YY1) zinc finger transcription factor binds this 37-bp enhancer within a protein complex. In addition to YY1's role as an initiator of tumorigenesis and inhibitor of important cell-cycle progression and tumor suppressor genes, there is mounting evidence that YY1 may also play a regulatory role in normal biological processes (Gronroos et al., 2004; Gordon et al., 2005; Wang et al., 2006). Further *in vitro* site-directed mutagenesis and *in vivo* deletion assays revealed that this 37-bp enhancer is necessary for *in vivo* Schwann and OFT endocardial cushion lineage reporter expression.

Both Schwann cell and OFT endocardial cushion morphogenesis are dependent upon neural crest morphogenesis (Jessen and Mirsky, 2002; Conway et al., 2000). Most Schwann cells are neural crest derived (Le Douarin et al., 1991) and undergo a defined series of developmental transitions that ultimately give rise to mature Schwann cells (Jessen and Mirsky, 2005). Following migration of a neural crest subpopulation and subsequent activation of the Schwann cell differentiation cascade, neural crest cells can give rise to Schwann cell precursors that then undergo a series of molecular and morphological changes to generate immature and finally mature myelinating and non-myelinating Schwann cells (Jessen and Mirsky, 2005). Similarly, a subpopulation of the cardiac neural crest lineage migrate and colonize the distal cardiac OFT endocardial cushions and then undergo a series of molecular and morphological changes that ultimately forms the septa between the aorta and pulmonary artery (Jiang et al., 2000; Conway et al., 2003). These results represent the identification and initial characterization of a novel enhancer element that modulates expression of *periostin* solely within the post-migratory OFT endocardial cushions and Schwann cell precursors of the developing mouse embryo.

Materials and methods

Bioinformatics analysis

Paired alignment and visualization of homology between mouse and human *PERIOSTIN* promoter sequence was undertaken using zPicture software (Ovcharenko et al., 2004; Loots and Ovcharenko, 2004). Multiple alignment of mouse (*NC_000069*), dog (*NC_006607*), human (*NC_000013*) and rat (*NC_005101*) *periostin* promoter sequences was accomplished using the ClustalW software (Thompson et al., 1994). Single polymorphic nucleotide analysis of *PERIOSTIN* upstream sequence revealed the presence of 2 well supported human SNPs (rs17197936a and rs17197908c; indicated in Fig. 6A).

Animal model

Periostin (*peri*^{lacZ}) knockin knockout mice generated previously (Rios et al., 2005) were maintained on a C57BL/6J genetic background and fed powdered Teklad LM-485 Complete Mouse Diet to alleviate runting. Tissue isolation, fixation and processing for *lacZ* staining was carried out as described (Rios et al., 2005). All animal experimentation was performed in accordance with

National Institutes of Health Guidelines, and protocols were approved by the Institutional Animal Care and Use Committee at IUPUI (Study #2707).

Generation of 3.9 kb$^{peri\text{-}lacZ}$ reporter mice

To begin to identify the *cis*-elements and *trans*-factors necessary and sufficient for *periostin* developmental transcriptional activity, we PCR cloned 3.9 kb of the 5′ mouse *periostin* promoter from a 92-kb 129SvJ mouse ES cell genomic DNAlibary bacterial artificial chromosome (clone#318a12, Genome System Inc., St. Louis, MO) using a high-fidelity Thermal Ace DNA polymerase kit (Invitrogen, Inc., Carlsbad, CA). Its identity and fidelity were confirmed by 4-fold coverage sequencing and overlaps NCBI *Mus musculus* chromosome 3 genomic clone #NT_039240. Primers used were as follows: sense (5′ GCgtcga-cCTAAGGTGGACAGTGCGGAAGAC-3) and antisense (CctcgagCTT-CAGCCCTGAGCTCCGTCC-3). The primers were engineered to produce a 5′ *Sal*I site (in lowercase letters) and a 3′ *Xho*I site (in lowercase letters), which enabled us to directionally clone the insert in frame into a promoterless IRES-nuclear localized β-galactosidase expression cassette. The resulting construct was either introduced as a 3.9-kb promoter that contains the 5′-UTR and promoter elements of *periostin* genomic DNA (up to but not including the ATG) or as a 5′ truncated 1.2-kb promoter (following digestion with an internal unique *Stu*I site). Following pronuclear injection, resultant embryos were transferred into pseudopregnant C57Bl/6 female oviducts. Resulting F_1 mice were screened by Southern blot, and positive males were bred to wild-type C57Bl/6 female mice. Two 3.9-kb$^{peri\text{-}lacZ}$ and four 1.2-kb$^{peri\text{-}lacZ}$ independent lines were produced, and F_2 germline transmission of the transgene was examined by both PCR and *lacZ* staining (Fig. 2).

Histological, in situ and immunohistochemical analysis

Microdissected embryos of various ages were either fixed briefly with 4% paraformaldehyde (PFA), flash frozen directly in OCT mounting media (Sakura Finetek, Torrance, CA) following 10%, 20%, 30% sucrose protection or directly stained for *lacZ* and examined as described (Rios et al., 2005). At least 5 embryos at each developmental stage were assessed for β-galactosidase reporter activity. Immunodetection of periostin (1:8,000 dilution), α-smooth muscle actin (1:5,000 dilution, αSMA, Sigma, St. Louis MO) and neurofilament-H (1:8,000 dilution, Chemicon) were performed as described (Kruzynska-Frejtag et al., 2004). Unfixed frozen embedded embryos were sectioned (10 μm), fixed briefly with 4% PFA, stained for *lacZ* and then washed in saline prior to protein blocking and incubation with a goat anti-Sox10 antibody (1:75 dilution, Santa Cruz Biotech, CA) and detection via rabbit anti-goat-FITC secondary antibody (1:100 dilution, Vector Labs, CA). Both sets of immunoassays were repeated at least 3 times.

Radioactive *in situ* hybridization detection of endogenous *periostin* expression was performed as previously described (Kruzynska-Frejtag et al., 2001). *Sox10* mRNA expression was detected using a cDNA probe, cloned via PCR amplification from E12.5 whole embryo cDNA using the following primers: 5′-TCTGTCTTCACCTGGGCTTT and 3′-ATGTCAGATGGGAACC-CAGA. The 420-bp *Sox10* PCR fragment was cloned into the pCRIITOPO vector (Invitrogen) and sequenced to verify identity and orientation. Both sense and antisense ^{35}S-UTP-labeled probes were generated, and specific signal was only observed when sections were hybridized with the antisense probe (repeated at least 3 times).

RT4-D6P2T cell line

RT4-D6P2T (RT4) rat Schwannoma cells (a kind gift of Dr. Pragna Patel, USC) were grown in DMEM (Gibco), supplemented with 10% fetal bovine serum and 100 U/mL penicillin and 100 μg/mL streptomyosin at 37 °C with 5% CO_2.

In order to characterize the RT4 cells and assess endogenous periostin expression, both RT4 and NIH3T3 (ATCC) lines were used. Additionally, newborn extracts ($n=3$) from wild-type and *peri^{lacZ}* null mice were used for Western analysis as described (Rios et al., 2005). For analysis, ~100 μg of cell lysate and medium (equal amounts for RT4 and NIH3T3) and ~80 μg newborn samples were resolved via 12% SDS–PAGE (Bio-Rad). Loading was normalized using a monoclonal anti-actin antibody (Sigma) at 1:5,000 dilution and the relative levels of periostin measured using our affinity-purified anti-periostin rabbit polyclonal antibody at 1:12,000 dilution (Kruzynska-Frejtag et al., 2004).

For immunohistochemical analysis, cells were grown on glass culture slides (LabTech, Nalge-Nunc Inc.), fixed briefly with 4% PFA and stained for periostin and Sox10 as described above ($n=3$). Anti-S100 staining was accomplished using the S-100 Immunohistology Kit (cat. IMMH-9, Sigma-Aldrich, St. Louis, MO). All images were taken using a Zeiss AxioSkop2 Plus.

Luciferase reporter constructs, mutagenesis, transfection and luminometry

The 3.9-kb proximal *periostin* promoter was directionally cloned into the promoterless pGL2-Basic vector (Promega Corp., Madison WI). The sequenced 3.9-kb^{peri}-pGL2 clone was then serially and internally deleted to generate a set of truncated constructs. In addition, site-directed mutagenesis of three mouse–human homology sites was accomplished using the GeneTailor Site-Directed Mutagenesis System in a pSKII Bluescript shuttle vector (Invitrogen Carlsbad, CA). Following sequencing verification of designed mutations, both a 804-bp and an internal 304-bp enhancer were excised and ligated into pGL2 vectors for reporter analysis.

Molar equivalents of each construct and 50 ng of the Renilla control plasmid (pRL-CMV, Promega) were co-transfected into RT4 cells using the Mirus TransIt-LT1 lipoamine reagent (Mirus Bio Corp. Madison, WI). Following 48 h incubation at 37 °C, protein lysates were harvested from transfected cells and accessed for luciferase activity using the Dual-Luciferase Reporter Assay System (Promega Corp.) Quantitative luminometry was performed using an Lmax luminometer (Mol. Devices, Sunnyvale, CA). Each transfection was performed three separate times in duplicate and each sample was read twice.

Electromobility shift assays (EMSA)

Nuclear extract was isolated from RT4 cells following a modified Dignam protocol (Dignam et al., 1983) and EMSAs performed as described (McFadden et al., 2000). Radioactive double-stranded DNA probes were generated from P^{32}-labeled complimentary single stranded oligos and purified by acrylamide gel purification. Cold probe was generated from the hybridization of unlabeled oligos. The sequences for the probes are listed in table below:

Site 1	5′-ATAATGAACCATTTCTTTCT-3′
Site 2	5′-TCAGTAATGACTTACATCT-3′
Site 3	5′-ACATCTCTGGGTCAGACTTT-3′
Site 12	5′-TAATGAACCATTTCTTTCTCAGTAATGACTTACATCT-3′
Site 123	5′-TAATGAACCATTTCTTTCTCAGTAATGACTTACATCTCT GGGTCAGACTTT-3′
Non-specific	5′-GCTCCACCGCCATCTCCGTATTA-3′
YY1 control	5′-ATGCCTTGCAAAATGGCGTTACTGCAG-3′
SRF control	5′-ACACAGGATGTCCATATTAGGACATCTGC-3′

Pure YY1 protein was generated from both pcDNA3-CMV-YY1 and pcDNA3-CMV-YY1-His-tagged full-length cDNA vectors using the TnT rabbit reticulocyte lysate expression system (Promega). Equivalent amounts of both YY1 and unprogrammed lysate were used in EMSA analysis to assess the ability of YY1 to bind the Site 123 probe listed above. Western blotting with the YY1-specific antibody (1:1,000 dilution; Santa Cruz) was used to verify that only programmed lysate contained YY1.

Generation of Hsp68-804$^{peri\text{-}lacZ}$, Hsp68-304$^{peri\text{-}lacZ}$ and Hsp68-3900$^{-37\ bp}$ transient F_0 transgenic analysis

Two DNA fragments, corresponding to −2924 to −2119 (804 bp) and −2509 to −2205 (304 bp) were isolated, blunted via Klenow and ligated into a minimal promoter-*lacZ* reporter vector, *Hsp68-lacZ* (Kothary et al., 1989; McFadden et al., 2000). The 37-bp enhancer, corresponding to −2373 to −2336 was deleted from the original 3.9-kb 5′-prime UTR and promoter fragment using the GeneTailor Site-Directed Mutagenesis System, to make the *Hsp68-*

$3900^{-37\ bp}$ mice. F_0 transgenic mice were generated by pronuclear injection of the various linearized transgenes (IU School of Medicine Transgenic Core Facility) and harvested at E12–13 gestational age. Following microdissection and isolation of limb buds for PCR genotyping, F_0 embryos were fixed, stained for *lacZ* and paraffin embedded for detailed histological analysis.

Results

Bioinformatic analysis

In order to better understand the mechanisms driving dynamic periostin expression *in utero*, we made use of comparative species sequence analysis. Such analysis is based on the concept that small non-coding sequences conserved between related species are likely the product of positive selection and often contain critical transcriptional regulatory elements. Cross-species comparison indicates that the majority of evolutionarily conserved domains were present within the proximal 4 kb of *periostin* upstream region relative to the location of the transcriptional start site. This putative *periostin* promoter sequence, designated 3.9 kb^{peri}, includes 3866 bp of the sequence immediately upstream of the transcriptional start site and 18 bps of non-coding exon 1. Comparative analysis reveals relatively homogenous distribution of highly conserved sequence between rat and mouse (86.2% identity). In contrast, when 3.9 kb^{peri} was aligned with more distantly related species such as dog and human, seven discrete focal peaks of high identity are revealed (data not shown). Interestingly, the peaks in the two non-rodent species were highly similar, both in term of degree of sequence identity and spatial distribution. As a number of possible *cis*-modules were identified within the proximal 4 kb of *periostin*, we tested their role directly by generating transgenic mice designed to drive expression of the β-galactosidase reporter via this conserved 3.9 kb^{peri} region.

Periostin proximal 3.9 kb promoter expression patterns

The 3.9-kb^{peri} sequence was cloned into a nuclear-localized β-galactosidase reporter vector. The resulting construct was either introduced as an intact 3.9-kb *periostin* promoter or as a 5′ truncated 1.2 kb *periostin* promoter (following digestion with a unique internal *Stu1* site). The 1.2-kb construct facilitated the *in vivo* assessment of a previously identified *in vitro Twist* binding site at position −468 bp (Oshima et al., 2002).

Two 3.9 kb$^{peri\text{-}lacZ}$ and four 1.2 kb$^{peri\text{-}lacZ}$ independent permanent mice lines were produced and their respective β-galactosidase reporter expression patterns examined. Transgenic analysis revealed that the 1.2-kb$^{peri\text{-}lacZ}$ promoter (all four lines) was not capable of driving any *lacZ* reporter expression *in vivo* at any stage during embryonic and extraembryonic development (E8-newborn stages examined; not shown). In contrast, spatiotemporal analysis of two independent 3.9 kb$^{peri\text{-}lacZ}$ lines revealed that *lacZ* reporter expression is present throughout the PNS, enteric nervous system and within a subpopulation of cardiac OFT endocardial cushion mesenchymal cells. In contrast to the relatively widespread endogenous *periostin* embryonic gene expression (Kruzynska-Frejtag et al., 2001; Kruzynska-Frejtag et al., 2004; Lindsley et al., 2005; Rios et al., 2005), 3.9 kb$^{peri\text{-}lacZ}$ expression is only present in restricted subpopulations. As both 3.9 kb$^{peri\text{-}lacZ}$ lines exhibited similar reproducible expression patterns and were both found in normal Mendelian

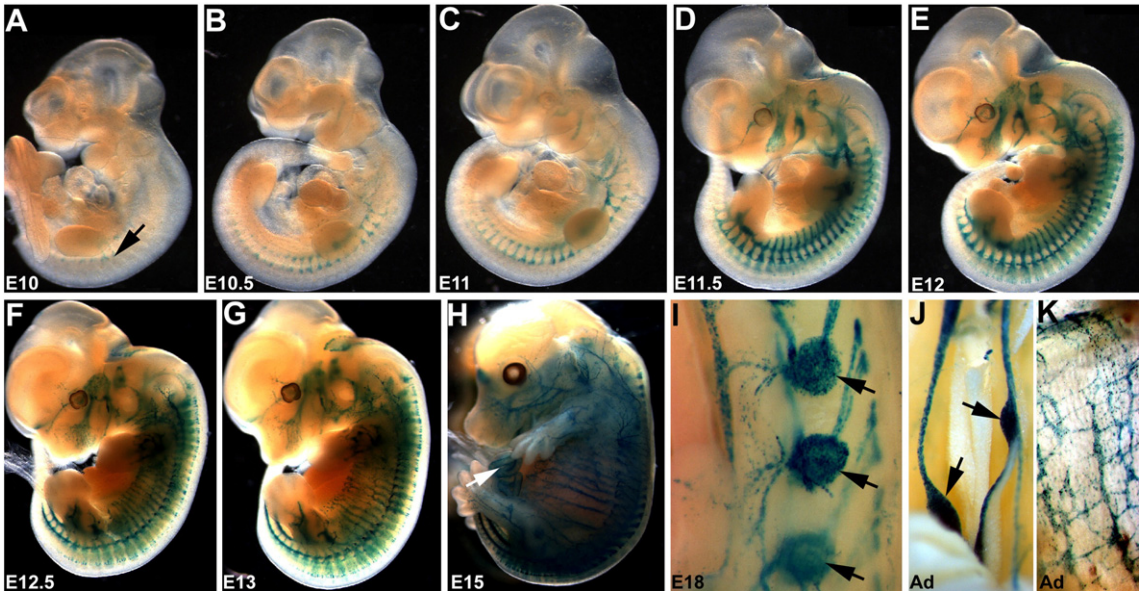

Fig. 1. Developmental expression pattern of 3.9 kb$^{peri\text{-}lacZ}$ transgenic reporter: Developmental series of mouse embryos E10–18 and adult organs stained to detect 3.9 kb$^{peri\text{-}lacZ}$ expressing β-galactosidase-positive cells using X-gal substrate (n=48). (A) Note expression begins at ~E10 in the trunk PNS adjacent to the forelimb (arrow in panel A) and continues throughout development as the staining intensity progressively increases (B–H). Weak 3.9 kb$^{peri\text{-}lacZ}$ expression can initially be detected in E11 facial ganglia and facial nerves (C). Robust punctuate 3.9 kb$^{peri\text{-}lacZ}$ expression is also present in E15 midgut enteric nervous system (arrow in panel H) and fetal dorsal root ganglia and corresponding nerves (arrows in panel I). Note that 3.9 kb$^{peri\text{-}lacZ}$ expression is absent from the CNS. Postnatally, 3.9 kb$^{peri\text{-}lacZ}$ expression is maintained in the left and right sympathetic trunks and ganglia (arrows in panel J) and in the network of adult enteric ganglia (K).

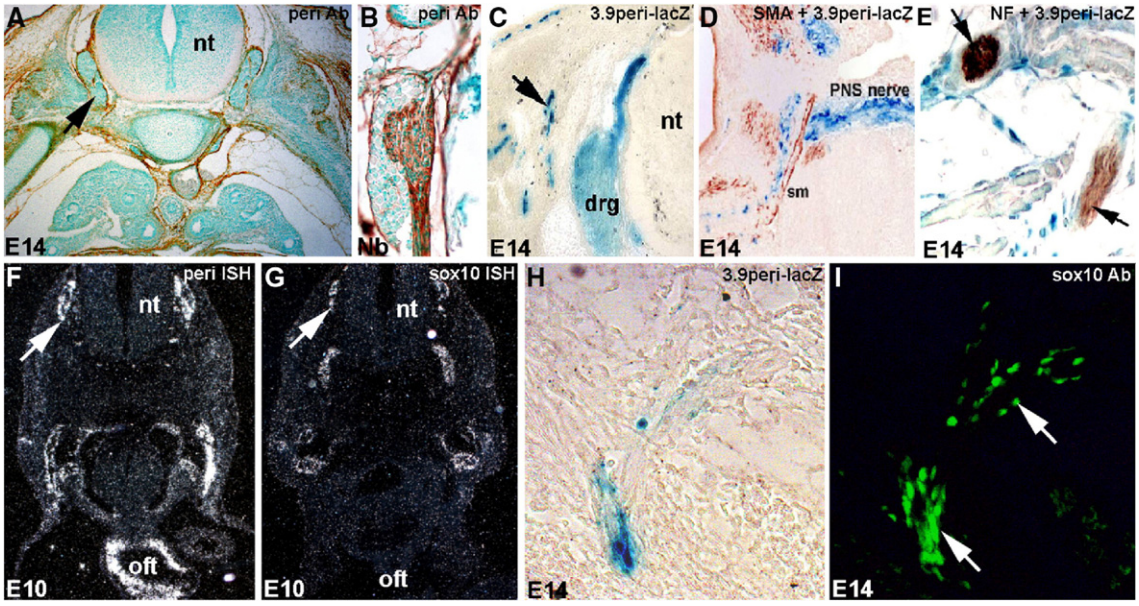

Fig. 2. The 3.9 kb$^{peri\text{-}lacZ}$ reporter is expressed in Schwann lineage. (A) Endogenous periostin protein is expressed in many E14 tissues and organs, particularly in periosteum and around dorsal root ganglia (arrow in panel A). Note that while periostin is expressed in many tissues, it is absent from the neural tube (nt). (B) In newborns, the dorsal root ganglia, its sheath and the nerve emanating from the ganglia are intensely labeled. (C–E) Sections of *lacZ* stained 3.9 kb$^{peri\text{-}lacZ}$ transgenic-positive E14 embryo reveals β-galactosidase-positive cells throughout dorsal root ganglia (drg) and along nerve tracks (arrow in panel C). Double labeling with α-smooth muscle actin (SMA) and neurofilament-H (NF) antibodies revealed that the *lacZ*-positive cells are neither smooth muscle or nerve cells, as both are mutually exclusively expressed. The 3.9-kb$^{peri\text{-}lacZ}$ expressing cells appear to surround the nerves, suggesting they are Schwann cells. (F and G) In order to verify that endogenous *periostin* and the Schwann cell marker *Sox10* transcription factor are co-expressed in the dorsal root ganglia, serial sections were probed with ^{35}S-labeled *periostin* and ^{35}S-labeled *Sox10 in situ* probes. While *Sox10* is restricted to dorsal root ganglia, sympathetic ganglia and the peripheral nerves; *periostin* is co-expressed with *Sox10* in the dorsal root ganglia (arrows in panels F and G) and is also present within the aortic arch arteries and OFT endocardial cushion cells (oft). (H and I) Identical section of an E14 3.9 kb$^{peri\text{-}lacZ}$ lacZ-stained embryo was subsequently probed with Sox10 antibody (which marks early Schwann cell precursors). Note co-expression of 3.9 kb$^{peri\text{-}lacZ}$ reporter and nuclear anti-Sox10 fluorescence (arrows in panel I).

ratios, subsequent analysis and data are derived from line #1 to ensure consistency.

Reporter 3.9 kb$^{peri\text{-}lacZ}$ expression is initially detected at E10 within the post-migratory pre-Schwann cell precursors. This makes the 3.9-kb^{peri} enhancer one of the earliest developmentally regulated Schwann cell promoters to date. The 3.9-kb$^{peri\text{-}lacZ}$ expressing cells radiate out from the presumptive dorsal root ganglia and encapsulate the developing peripheral nerves (Fig. 1), including the enteric nerves of the developing gut, establishing the *periostin* promoter as a novel Schwann cell *in vivo* marker (Fig. 1). Robust reporter expression in the Schwann cells is maintained throughout embryogenesis, perinatal development and into adulthood (Fig. 1), indicating that both *periostin* and 3.9 kb^{peri} enhancer expression are maintained during transition of the neural crest-derived precursor into mature Schwann cells. The validity of the reporter expression as well as the identity of the stained cells was established by marker gene analysis and co-localization of 3.9 kb$^{peri\text{-}lacZ}$ expression with the Schwann cell marker *Sox10* transcription factor (Fig. 2) (Britsch et al., 2001). Thus, the 3.9-kb$^{peri\text{-}lacZ}$ promoter is unable to completely recapitulate endogenous *periostin* expression (Fig. 2) but is capable of driving reporter expression within a subpopulation of endogenously expressing *periostin* cells. This is consistent with the hypothesis that modular *cis* elements coordinately regulate complex gene expression patterns (Firulli and Olson, 1997).

In addition to Schwann cell expression, mesenchymal cells of the cardiac OFT cushions also exhibit 3.9 kb$^{peri\text{-}lacZ}$ expression. At E10, a few individual *lacZ*-positive cells can be detected in the truncal region of the OFT (Fig. 3). Coincident with initiation of mesenchymal condensation and OFT

Fig. 3. 3.9 kb$^{peri\text{-}lacZ}$ reporter is also expressed in the developing heart. Developmental series of 3.9 kb$^{peri\text{-}lacZ}$ mouse embryo hearts (A–F) and a heterozygous knockin *peri*^{lacZ} heart (G and H). Isolated *lacZ*-stained 3.9 kb$^{peri\text{-}lacZ}$ whole hearts at E10 (A), E11 (B), E12 (C) and E14 (D). Black arrows indicate location of 3.9 kb$^{peri\text{-}lacZ}$ expressing cells. Note speckled expression begins at ~E10.0 within the OFT and expression increases as development proceeds. (C) Two robust streams of *lacZ*-positive cells are restricted to the truncal region of the E12 OFT endocardial cushions (indicated by arrows). Also note the 3.9-kb$^{peri\text{-}lacZ}$ reporter is restricted to the OFT and not present in AV region (inset in panel C in rear view of heart shown in panel C). (D) The two lacZ-positive streams resolve into a single clump at the base of the E14 OFT, coincident with completion of OFT septation and interventricular septal closure. (E and F) Eosin counterstaining of sections through the truncal and AV regions of the 3.9-kb$^{peri\text{-}lacZ}$ heart shown in panel C. Note that 3.9 kb^{peri} *lacZ*-positive cells are present in the mesenchymalizing OFT cushion septum (E) but are absent from the surrounding myocardial cuff and overlying endothelial cells. (F) No 3.9-kb$^{peri\text{-}lacZ}$ *lacZ* expression is detectable in AV cushions (indicated by arrow). (G and H) Whole-mount E12 heterozygous knockin *peri*^{lacZ} hearts stained for lacZ reveal that endogenous *periostin lacZ* reporter is robustly expressed in both the OFT (large arrow in panel G, heart viewed from front) and the AV endocardial cushions (large arrow in panel H, heart viewed from back). Abbreviations: RV=right ventricle; LV=left ventricle; Ao=aortic orifice; P=pulmonary orifice.

septation, additional *lacZ*-positive cells are seen at E11 and by E12 two robust streams of 3.9 kb$^{peri\text{-}lacZ}$ expressing cells can be observed in the aortic and pulmonary conotruncal endocardial cushions. By E14, these streams have resolved into a small clump of *lacZ*-positive cells at the base of the OFT. Significantly, *lacZ* staining revealed that the 3.9-kb$^{peri\text{-}lacZ}$ expression in the OFT is uniquely restricted (Fig. 3). While knockin *peri*^{lacZ}, *periostin* mRNA and protein are all detected throughout both the proximal and distal OFT and atrioventricular (AV) cushions, 3.9 kb$^{peri\text{-}lacZ}$ reporter expression is restricted to a subpopulation of distal OFT endocardial cushion cells. This indicates that elements required for AV cushion

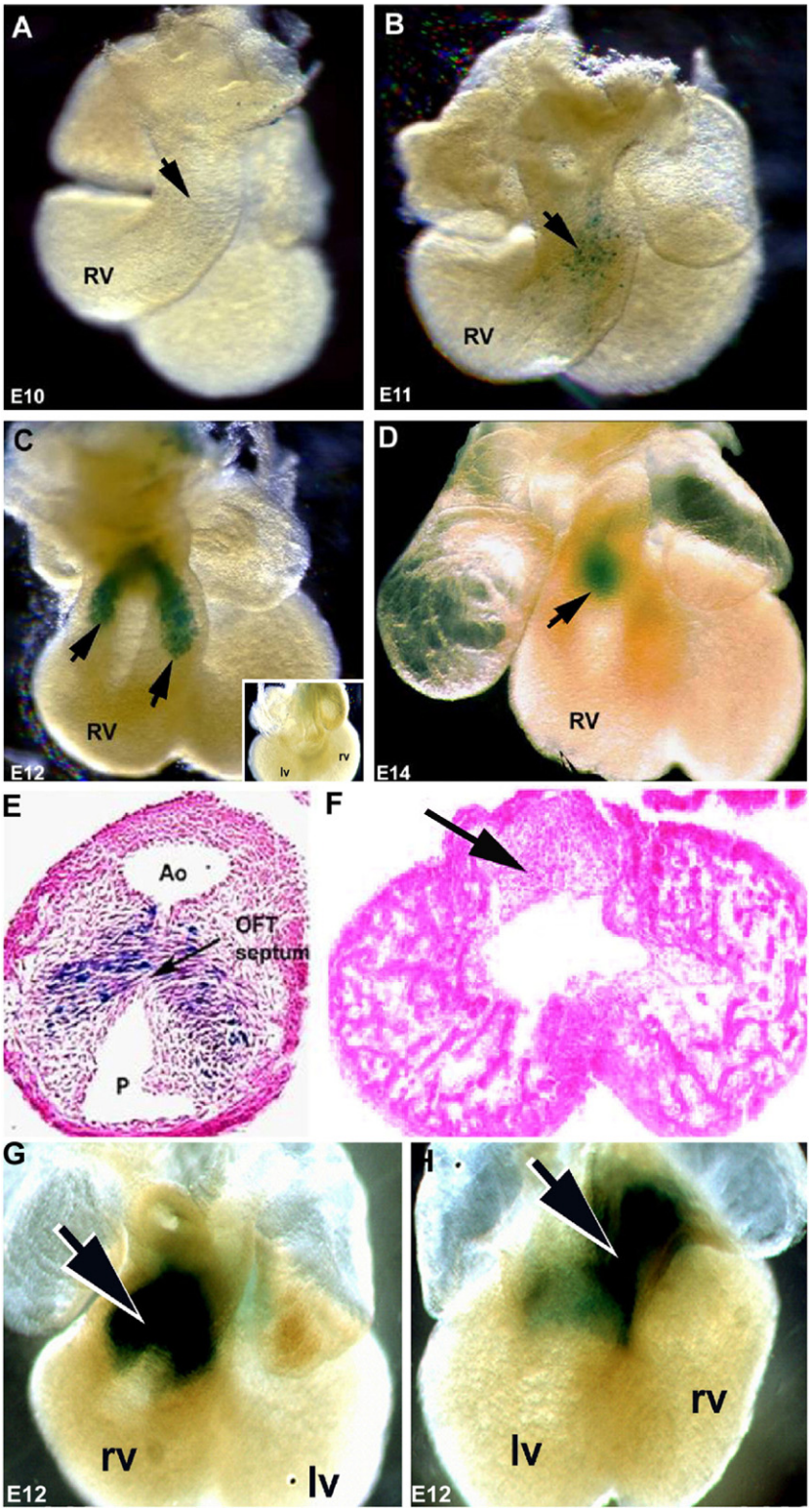

expression are absent from the 3.9-kb promoter and may lie outside the 3.9-kb domain. Together these data indicate that a subset of *cis*-regulatory elements reside within the proximal 4 kb of mouse *periostin* and that these elements drive expression in Schwann cells and the cardiac OFT. To further refine the location of these *cis*-elements we initiated *in vitro* analysis using a Schwannoma cell line.

RT4-D6P2T Schwannoma cell line characterization

While transgenic analysis is unrivaled in its ability to characterize promoter activity in all of the tissues of a developing embryo, the technique is not practical for the systematic identification of smaller regulator modules within a putative promoter. In contrast, cell culture-based methods have been highly successful alternatives to exhaustive and expensive *in vivo* transgenic analysis. Unfortunately, cell culture approaches require the availability of cell lines ontologically appropriate for the expression pattern of the gene of interest. Given the correlation of aberrant *periostin* expression in multiple neoplasias and the robust and sustained 3.9 kb$^{peri\text{-}lacZ}$ reporter expression in the PNS, plus the current lack of availability of any suitable endocardial cushion cell line, we used the well characterized RT4-D6P2T (RT4) rat Schwannoma cell line (Toda et al., 1994; Hai et al., 2002). Schwannomas are benign nerve sheath tumors composed of abnormally proliferating Schwann cells. RT4 cells have successfully been used for the molecular analyses of myelin and other PNS-specific promoters (Madison et al., 1996; Gonzalez-Martinez et al., 2003). Prior to molecular dissection of the 3.9-kb *periostin* promoter and to verify whether the RT4 cells would be useful within our system, marker analysis was performed and *periostin* expression examined. Western blotting reveals that RT4 cells normally express periostin and moreover they express both ECM-bound and secreted isoforms, analogous to those expressed by mouse *in vivo* (Fig. 4A). The cell line also proved to be immunopositive for S-100, a cytoplasmic EF-hand calcium binding protein (Jessen and Mirsky, 2002) found predominately in Schwann cells and other glial elements (Fig. 4B). Immunofluorescent detection of the HMG-containing transcription factor Sox10, a Schwann cell marker (Ye et al., 1996; Kuhlbrodt et al., 1998; Britsch et al., 2001), revealed a strong, nuclear localized signal in RT4 cells (Fig. 4C). Finally, the RT4 cell line is also positive for periostin protein within the cytoplasm, thus confirming that our gene of interest was actively expressed by our *in vitro* model system and therefore appropriate for promoter analysis (Fig. 4D).

3.9 kb^{peri} deletion analysis

To facilitate the identification of specific regulatory elements, we cloned the 3.9 kb^{peri} enhancer into the promoterless

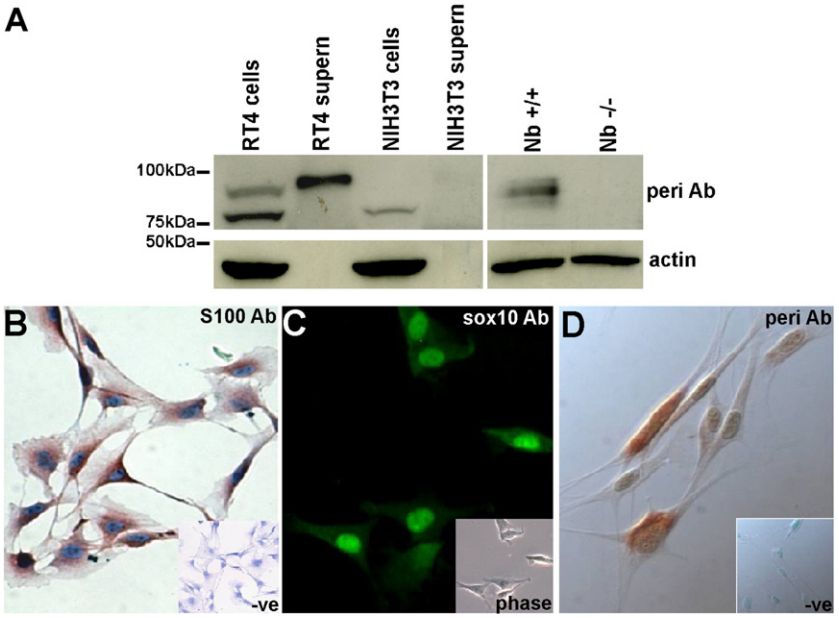

Fig. 4. RT4-D6P2T characterization: (A) Western analysis revealed the RT4 Schwannoma cell line, as opposed to NIH3T3 fibroblast line, expresses the higher molecular weight secreted periostin isoform, similar to the multiple isoforms expressed endogenously *in vivo* in newborn mice pups. While RT4 cells predominantly express two isoforms (~90 kDa and ~82 kDa) and RT4 supernatant contains secreted (~90 kDa) periostin, the NIH3T3 cells only express the lower molecular weight (~82 kDa) isoform within the cells and do not secrete periostin. Note that there is also a complete absence of periostin in the newborn nulls, verifying antibody specificity. Equal loading was ensured via normalizing for actin levels and loading equivalent amounts of supernatant (verified via Coomassie blue staining, not shown). (B–D) RT4 cells were grown on uncoated glass culture slides and briefly fixed with 4% PFA prior to immunostaining. (B) Anti S-100 staining, with hematoxylin nuclear counterstaining. Note cytoplasmic S-100 expression and absence of specific signal in negative control that did not receive the primary antibody (inset in panel B). (C) Anti-Sox10 immunofluorescent staining. Note appropriately localized Sox10 expression in nucleus and same view as phase-contrast (inset in panel C). (D) Anti-periostin staining, with methyl green nuclear counterstain and DIC optics. Note expression of periostin localized to the cytoplasm and that no expression is evident in negative control stained with pre-immune in place of primary periostin antibody (inset in panel D). The absence of staining in negative (−ve) control samples demonstrated that staining was specific. Magnification: all images 400×.

pGL2-Basic firefly luciferase construct. Serially truncated and internally deleted daughter constructs were all derived from the pGL2-3.9 kb^{peri} plasmid (Fig. 5). Transfection efficiency was controlled for by co-transfection of a Renilla luciferase expression plasmid.

The resulting luciferase reporter data revealed both activating (α, alpha) and repressing (β, beta) elements within the *periostin* proximal promoter (Fig. 5A). Construct A contains the 3.9-kb^{peri} sequence. When compared to cells transfected with the promoterless pGL2 parent vector, construct A generates a luciferase activity ~500-fold stronger, indicating the presence of the *periostin* transcriptional start site and putative *cis*-elements (data not shown). Deletion of 942 bp from the 5′ prime end (construct B) results in a 35.3% drop in luciferase activity, while a more significant 77.7% drop was observed when an additional 498 bp was removed (construct C). Additional truncation (constructs D–G) did little to further reduced luciferase reporter activity, suggesting that the reporter activity represents the baseline level of transcription from the *periostin* promoter. Deletion of the putative TATA box further reduced levels of expression comparable to that observed with pGL2-Basic vector only, supporting this conclusion (data not shown). Serial deletion analysis therefore suggested that the most potent transcriptional activation domains were contained in the most 5′ prime 1.4 kb of the 3.9-kb^{peri} sequences, consistent with our 3.9 kb^{peri} (Fig. 1) and 1.2 kb^{peri} *in vivo* transgenic data.

We next engineered additional constructs with internal deletions and assessed resultant reporter activity (constructs H-J). To further characterize the 5′ prime 1.4-kb element(s), we first removed an internal DNA fragment from −2119 to −1287. This construct (construct H) shows an increased luciferase activity of ~80% compared to the activity of 3.9 kb^{peri} (construct A) suggesting the presence of a possible transcriptional repressor element. A similar level of transcriptional activity was observed when construct H was further truncated by the removal of its distal 942 bps (construct J); however, removal of a larger 1637-bp internal fragment (construct I) reduced luciferase activity to the levels observed with construct

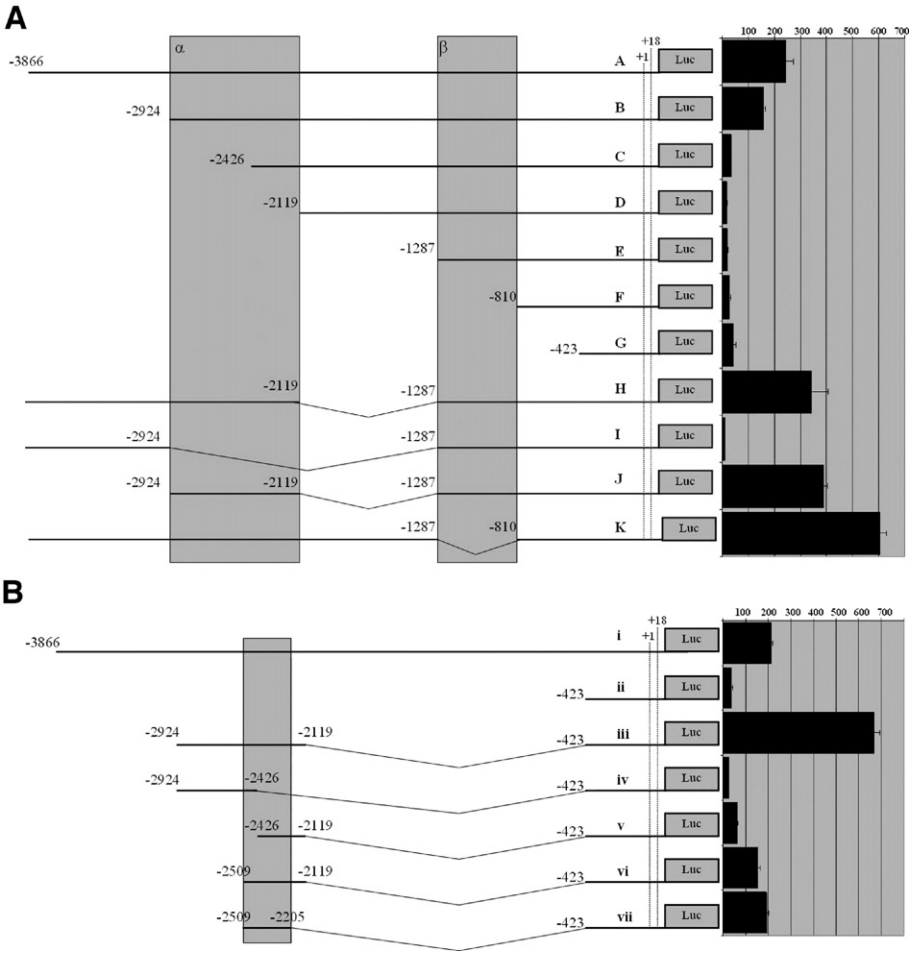

Fig. 5. *In vitro* analysis of 3.9 kb^{peri} enhancer: (A) Serial and internal truncation of 3.9 kb^{peri}-pGL2 construct and luminometry results. Schematic of constructs are shown with nucleotide assignment given relative to the transcriptional start site (+1). Sequence includes 18 bp of exon one, up to, but not including the ATG translational start site. (α, alpha) Corresponds to an 804-bp putative enhancer region from −2924 to −2119 bps upstream of the transcriptional start. (β, beta) Corresponds to a 477-bp putative repressor region from −1287 to −810 bps upstream of the transcriptional start. (B) Dissection of 803 bp^{peri} putative enhancer region. Schematic alignment of the sequences of truncated enhancer-minimal promoter fusion constructs and intact 3.9 kb^{peri}-pGL2 plasmid. Black bars represent the average of six independent transfections (n=6), while error bars represent the standard error. Lysates from each transfection were read twice and the results averaged. Luminometry results are given in arbitrary units.

G. These results suggest the existence of a transcriptional enhancer within the 804-bp segment of DNA spanning −2924 to −2119 region. A 477-bp internal deletion (construct K), was also found to significantly increase luciferase activity from that observed with construct A, suggesting that these sequences may contribute to the negative regulation of *periostin*.

In order to further define the putative *cis*-element, we designed a set of constructs that isolated the enhancing 804-bp fragment from other regulatory elements within the full-length 3.9 kb^{peri} while preserving the DNA elements need to drive the basal transcription. This strategy utilized the minimal promoter region corresponding to the 423 bps immediately upstream of the transcriptional start site. The putative 804-bp enhancer element was fused to the 5′ end of the minimal promoter element and its transcriptional activity assessed (Fig. 5, construct iii). An 18.8-fold increase in luciferase reporter activity is observed. Subsequent truncation of the 804-bp fragment (constructs iv–vii) results in decreased luciferase activity. Nevertheless, a moderately enhancing 304-bp core fragment (−2509 to −2205) was identified within the larger 804-bp fragment, which was sufficient to drive luciferase expression at a level equivalent to that observed for 3.9 kb^{peri} promoter. Significantly, sequence identity bioinformatics of the 3.9-kb^{peri} promoter revealed that this 304 bp (−2509 to −2205) fragment is localized within the region that contains the highest level of evolutionary conservation (72.94%). Table 1 is a bioinformatics representation of all known and conserved *cis*-elements within the 304-bp^{peri} minimal enhancer. To further refine our analysis of these regions, we carefully examined conserved and aligned sequences within the 304-bp fragment. Three highly conserved putative transcription factor-binding sites (highlighted in yellow) were identified and targeted for additional analysis (Fig. 6A).

Table 1
Bioinformatics representation of known and conserved *cis*-elements within the 304-bp minimal enhancer

(−2509 bp)
tggtgagtaagcgtggcagtgtaatgaccʳtcatggtctcccgag
gccagataacagagaacgtgcctataaatcagcatgccgcggct
agagagaaacggccctgtttctcagacacactatctʳctcttcagc
tacataatgʳaaccatttctttctcagtaatgʳacttacatct
ctgggtcagactttgcagccctggaaagtcggacttcattttcatʳg
atttccgtcatcttcccgactggtaggaaaattgcagggtcagta
gtgtcagcatagtttcacagaggctgaagagaaagggccc
(−2205 bp)

Activator Protein 1 (AP-1) | Isl-1 | Gata site | Smad binding element
Oct Canonival site | Retinioc Acid Response Element (RARE)

Cis-element scan analysis was performed using the MatInspector program, (Genomatix http://www.genomatix.de/) on the 304-bp^{peri} enhancer contained within −2509 to −2205 bps of 3.9 kb^{peri} promoter (note necessary 37 bp fragment is underlined and YY1 elements are indicated via enlarged text). The optimized matrix threshold was set to minimize false-positive hits, and only the highest conserved consensus binding sites (each >0.8) are indicated (note: a perfect match to the matrix scores 1.00, while strong candidates typically show a similarity of >0.80). The sequence that corresponds to each of the identified *cis*-elements is denoted on 304-bp^{peri} enhancer via the color-coded key. An "r" superscript indicates that the element is in reverse orientation in relation to the start site. Potential interesting elements identified include several *Gata* sites and retinoic acid response elements, an *Oct* consensus site and pancreatic/intestinal Lim-homeodomain factor (*Isl1*) and *activator protein-1* (*AP-1*) sites found within the 37-bp fragment. *Ap-1 has* been shown to play a critical role in Schwann cells differentiation (Miskimins and Miskimins, 2001; Wegner, 2000) and the myocardialized OFT septum has recently been shown to be derived from *Isl1*-expressing cells (Sun et al., 2007).

Enhancer mutagenesis

Using site-directed mutagenesis, we fused the 804-bp enhancer to the *periostin* minimal promoter (construct iii) and then disrupted the three most highly conserved modules identified by bioinformatic analysis (Fig. 6B). Mutation of site 1 and site 2 reduced luciferase activity by ∼80% and ∼65%, respectively, while mutation of site 3 had a minimal effect (∼17% reduction). Mutation of site 1 reduced luciferase activity nearly to basal levels, implying that a necessary *trans*-activator(s) requires the *cis*-elements of site 1's sequence in order to bind and drive transcription. The less dramatic reduction observed via mutation of site 2 may imply the binding of factors which moderately enhance *periostin*'s transcription. Although these data suggest we have further isolated the *cis*-elements within the 3.9 kb^{peri} promoter, validation was required to be sure that these elements function *in vivo*.

Transient F_0 transgenic analysis

Given the predictions provided by the *in vitro* analysis of the promoter, we sought to validate our findings *in vivo*. Both the 804-bp and 304-bp putative enhancer elements were cloned into an *Hsp68-lacZ* minimal promoter construct and were used to generate F_0 transgenic embryos. At E12.5 (stage at which 3.9 kb^{peri} reporter expression is maximal in PNS and OFT), both the *Hsp68*-804 bp$^{peri\text{-}lacZ}$ ($n=11$) and the *Hsp68*-304 bp$^{peri\text{-}lacZ}$ ($n=6$) positive embryos yielded Schwann cell expression throughout the developing PNS (Fig. 7). Intriguingly, both constructs yielded embryos that were uniformly *lacZ* positive in the mesenchymal cells of the distal OFT cardiac cushion while only individual, isolated *lacZ*-positive cells were observed to sparsely populate the AV cushion (Fig. 7B). Histological analysis revealed that *lacZ* expression was restricted to the mesenchyme of the distal OFT cushion, while the overlying endocardium and surrounding myocardium were negative (Figs. 7B and C). When compared to the 3.9-kb$^{peri\text{-}lacZ}$ expression pattern (see Fig. 3), the expression patterns of *Hsp68*-804 bp$^{peri\text{-}lacZ}$ and the *Hsp68*-304 bp$^{peri\text{-}lacZ}$ are both more extensive in the cardiac cushions, however, they are not ectopic in nature. As endogenous *periostin* mRNA and protein expression can be found throughout the proximal and distal OFT and AV cushion mesenchyme (Kruzynska-Frejtag et al., 2001; Lindsley et al., 2005; Litvin et al., 2005), this suggests that different enhancers may regulate endocardial cushion *periostin* expression in different cushions and within different regions of each cushion. Given the probable repressive element within the proximal region of 3.9 kb^{peri}, the less restricted expression patterns of *Hsp68*-804 bp$^{peri\text{-}lacZ}$ and *Hsp68*-304 bp$^{peri\text{-}lacZ}$

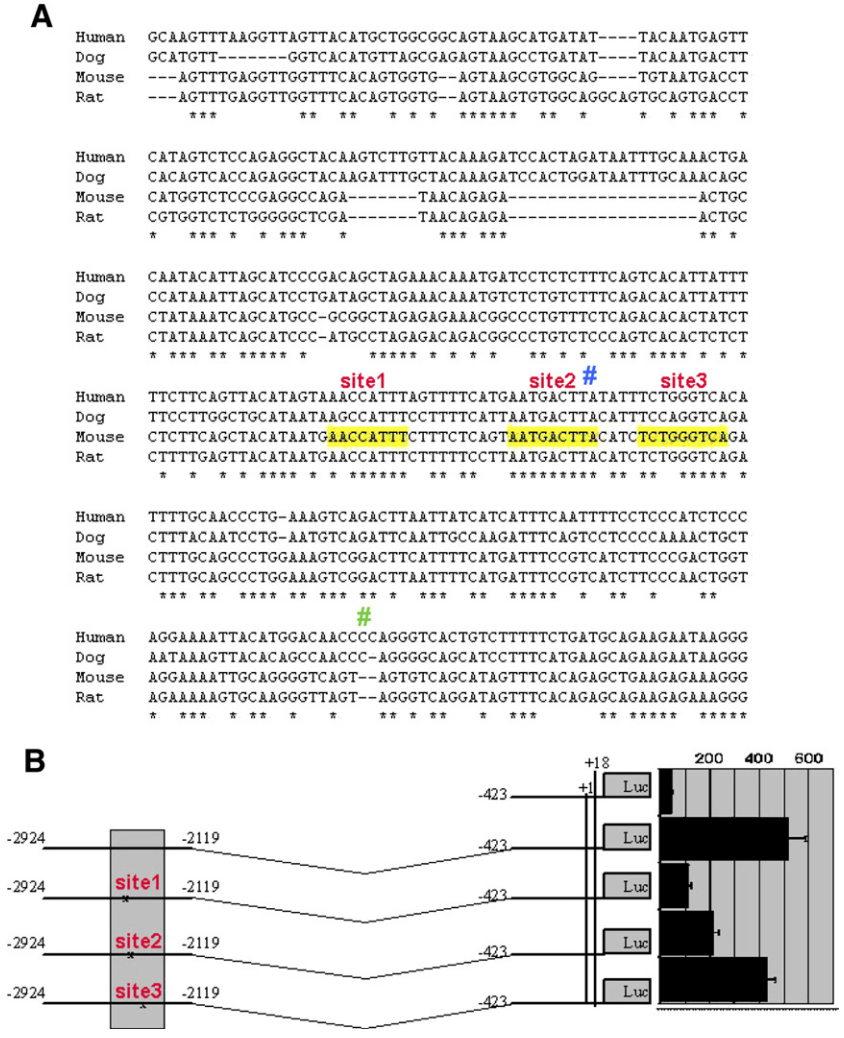

Fig. 6. Bioinformatic analysis of conserved sequences: (A) ClustalW multiple alignment of mouse (−2430 to −2126 bps upstream region), rat, dog and human DNA sequences. There are three highly significant evolutionary conserved regions of sufficient size to be potential transcription factor binding sites (highlighted in yellow). Two single-nucleotide polymorphisms (indicated by #) are present in the 304-bp enhancer, one is present within the 37-bp fragment (blue #). (B) All three sites (designated sites 1, 2 and 3) were targeted for subsequent site-directed mutagenesis. While mutation of site 3 had little effect, mutation of sites 1 and 2 both significantly reduced luciferase reporter activity in RT4 cells when compared to control 804 bp ^{peri} enhancer ($n=6$). Specifically, mutation of site 1 reduced luciferase to basal levels ($n=6$). The less dramatic reduction noted in the mutation of site 2 may imply the binding of factors acting synergistically or with factors that also bind site 1.

may be secondary to the removal of a negative putative regulatory element.

Protein–DNA interaction analysis

To assess the protein binding capacity of the identified *periostin* enhancers, 20-bp ^{32}P-radiolabeled double-stranded DNA probes where generated for sites 1–3 and electromobility shift assays (EMSAs) were performed. Each probe contained a single identified site and a minimum of 5 bp of upstream and downstream flanking sequence. Surprisingly, incubation with RT4 nuclear extract failed to retard the migration of any of the individual 20 bp probes (Fig. 8B). In contrast, when a probe encompassing all three sites (52 bp in total length) was incubated with the same RT4 nuclear extract, two prominent shifted bands (complex A, B) and one faint higher shifted band (complex C) were detected (Fig. 8C). The use of unlabeled "cold" probe successfully reduced the intensity of all three bands in a dose-proportionate manner whereas a non-specific DNA sequence of similar length has no such effect. Given that mutation of site 3 had little effect on promoter luciferase activity (Fig. 6B), we designed a probe 37 bp in length to examine the protein-binding capacity of just sites 1 and 2 (Fig. 8D). Results demonstrate that both the 52-bp (sites 1, 2 and 3) and 37-bp (sites 1 and 2) EMSA probes are specifically bound by RT4 nuclear extract proteins (whereas single site 20-bp probes did not) and that they yield a similar distribution of three DNA–protein complexes, each with discrete migratory properties.

To identify the nucleotides critical for DNA–protein complex formation, we individually mutated sites 1 and 2 within our 37 bp probe. We found that mutating either site altered stoichiometry of the three complexes. However, none of the bands were lost. Mutation of site 1 enhanced the intensity of the lowest band (complex A), while the faint higher band became hyper-intense following mutation of site 2 (complex C). These results suggest either the binding of the proteins that

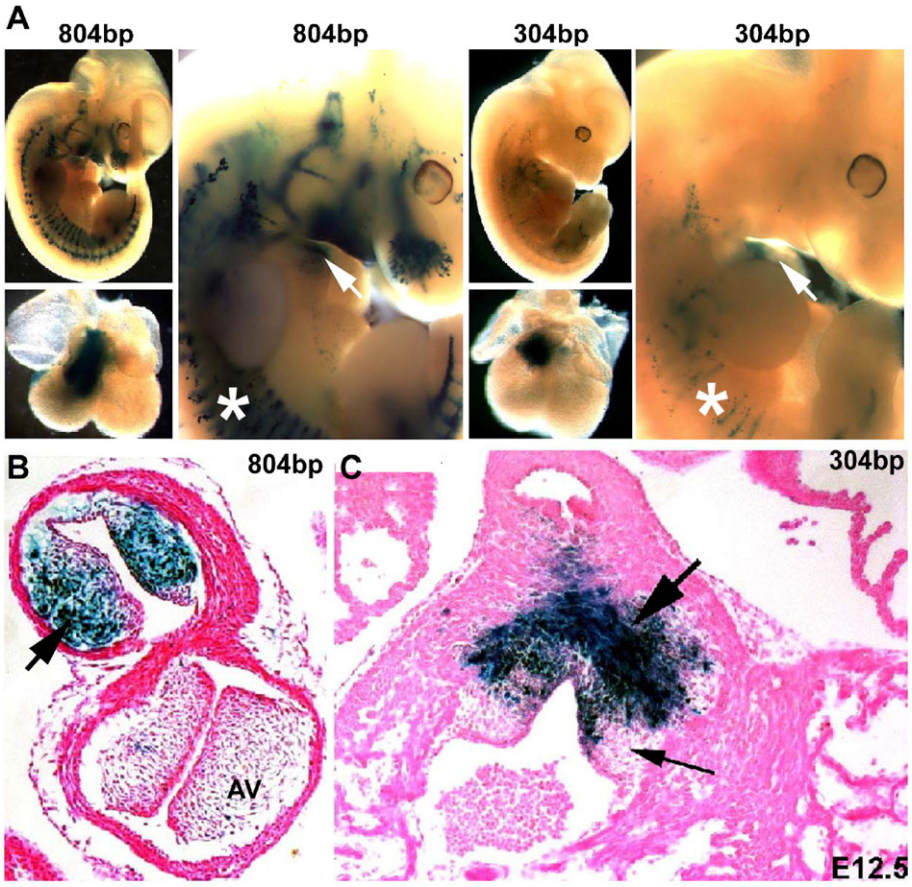

Fig. 7. Transgenic F_0 analysis of *periostin* enhancer expression. (A) E12.5 whole embryos and isolated hearts stained for *lacZ* reporter activity. First three panels illustrate F_0 transient transgenic pattern driven by 804 bp^{peri} enhancer ($n=11$), while next three panels illustrate F_0 304 bp^{peri} enhancer expression ($n=6$). Note that the 804-bp$^{peri\text{-}lacZ}$ enhancer recapitulates 3.9 kb$^{peri\text{-}lacZ}$ PNS (indicated by *) and OFT reporter patterns, and in fact 804 bp$^{peri\text{-}lacZ}$ OFT levels may even be enhanced as *lacZ* expression is now present within the most of the truncal and conal endocardial cushion cells. However, 304 bp$^{peri\text{-}lacZ}$ PNS *lacZ* expression is markedly reduced (indicated by *) while OFT expression is still robust, although restricted to the truncal region. (B) Histological sectioning reveals that 804 bp$^{peri\text{-}lacZ}$ reporter expression is confined to the endocardial cushions within the OFT (arrow). Note that some AV cushion expression is now evident, suggesting loss of repression. (C) Histological sectioning reveals that 304 bp$^{peri\text{-}lacZ}$ expression is also restricted to endocardial cushion cells but is absent in the adjacent myocardial cuff and endothelial cells. Note 304 bp$^{peri\text{-}lacZ}$ expression is present in truncal cushions (large arrow in panel C) but is absent in the conal region (small arrow in panel C).

constitute complex C is enhanced by the disruption of a specific sequence within the probe (i.e. site 2), or binding is mutually exclusive and factors compete for DNA access. Such an observation supports the notion that multiple proteins are cooperatively (perhaps acting synergistically) and/or antagonistically binding the probe. As a gel shift was only observed when the individual 20-bp fragments that failed to bind were combined, it is more likely that multiple factors bind cooperatively rather than antagonistically. Thus, each complex represents the averaged migrational properties of a specific combination of proteins.

Bioinformatic analysis of the 37-bp fragment identified two putative *YY1* transcription factor consensus binding sites (Flanagan et al., 1992; Ye et al., 1994; Yarden and Sliwkowski, 2001) overlapping sites 1 and 2. In order to assess the affinity of RT4 nuclear extract proteins for the YY1 consensus binding site, a competition assay was performed. A control probe containing a previously published YY1 consensus site was labeled and incubated with RT4 nuclear extract and a strong band was noted that was specific and could be ablated by the addition of cold YY1 probe (data not shown). When this non-radiolabeled YY1 control probe was co-incubated with a radiolabeled 37-bp fragment and RT4 nuclear extract, complexes A-C were significantly reduced in intensity (Fig. 8D, lane 5) suggesting specific competition. As YY1 and serum response factor (SRF) are known to be able to compete for similar binding sites (Lee et al., 1992; Flanagan et al., 1992; Ye et al., 1994; Yarden and Sliwkowski, 2001), we used an unlabeled SRF probe to test whether SRF bound the 37-bp probe. However, co-incubated cold SRF had no significant effect on complex formation (Fig. 8D, lane 6). These results suggest proteins that participate in the formation of complexes A–C also bind the YY1 control probe, but not the SRF control probe.

To directly test the ability of YY1 to bind the 37-bp probe, rabbit reticulocyte lysate was used to generate pure recombinant YY1 protein, both with and without a 3′ prime poly-histone tag. The identity of the recombinant YY1 was confirmed by Western blot (Fig. 8E). When co-incubated with labeled 37-bp probe, a prominent band was generated, demonstrating that YY1 protein

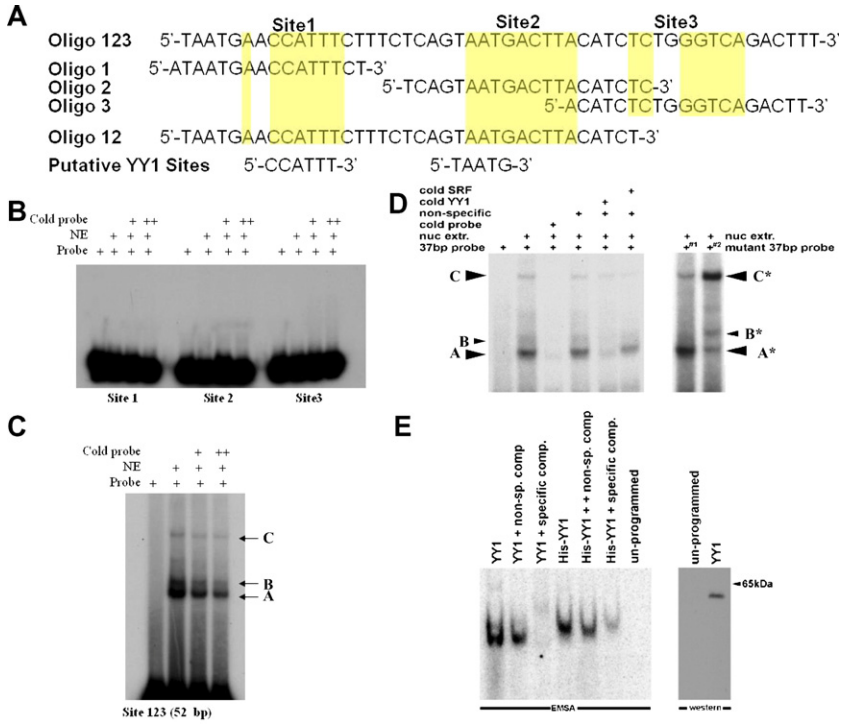

Fig. 8. Biochemical analysis of 304 bp^{peri} enhancer: (A) Annotated schematic illustrating alignment of various EMSA oligonucleotide probes containing conserved sites 1, 2 and 3 (highlighted in yellow). Oligo123 is a 52-bp probe containing all three sites of homology. Aligned below are the sequences of Oligo1, Oligo2 and Oligo3, each represents a 20-bp probe centered on a specific site of homology. Oligo12 is a 37-bp probe containing just sites 1 and 2. Putative YY1 transcription factor binding sites are aligned below to reveal their inclusion or exclusion within the various probes. (B) ^{32}P-labeled 20 bp double-stranded DNA probes as described above were hybridized with 3 μg of RT4-derived nuclear extract and cold probe. Note the absence of any bands for all three 20-bp probes, indicating that none of the probes alone is sufficient to generate DNA–protein complexes. (C) In contrast, when ^{32}P-labeled Oligo123 is co-incubated with the identical nuclear extract, 2 prominent bands and 1 faint band are generated (denoted as complexes A, B, C). Note that there is a dose-dependent competition of bands with unlabeled cold probe. (D) EMSA analysis of 37 bp fragment. ^{32}P-radiolabeled 37 bp probe was generated equivalent to Oligo12. Incubation with RT4 nuclear extract resulted in one prominent shifted band and two faint higher shifted bands (arrowheads, denoted as complexes A, B and C). Note that competition with specific cold competitor abolished all bands, while non-specific cognate probe had negligible effects. Significantly, given the presence of a YY1 binding site, cold YY1 probe greatly diminished bands while cold SRF probe had minimal effect. Site-directed mutation of either site 1 or site 2 resulted in alerted stoichiometry/intensity of the bands but did not abolish presence of any shifted bands (complexes A*, B* and C*). (E) EMSA analysis of 37-bp fragment with YY1-programmed extracts. Pure YY1 protein was generated from pcDNA3-CMV-YY1 full-length cDNA vector using TnT rabbit reticulocyte lysate expression system (Promega). Unprogrammed lysate failed to retard the migration of the 37-bp probe, while both His-tagged YY1 (slightly larger due to his tag) and YY1 alone resulted in shifted bands. Western blotting with YY1-speific antibody was used to verify that only the programmed lystate contained YY1 protein.

directly binds this sequence of the 3.9-kb^{peri} promoter. Given YY1's nearly ubiquitous expression, these data support the notion that YY1 participates in a complex of proteins driving 3.9 kb^{peri} expression patterns.

In vivo site-directed mutagenesis transgenic analysis

Having identified evolutionarily conserved YY1 cis-elements in the isolated 37-bp element present within the transcriptionally active *Peri*^{304} fragment, we set out to determine if the 37 bp were specifically necessary for any part of the observed 3.9-kb$^{peri\text{-}lacZ}$ expression. We therefore deleted the 37-bp from the 3.9-kb$^{peri\text{-}lacZ}$ construct and used it to generate F_0 transgenic litters (designated $3900^{-37\ bp}$). Our analysis revealed that deletion of the 37-bp site ablated all *in vivo lacZ* reporter expression (n=5/5; Fig. 9). This result demonstrates that the 37-bp site is a necessary enhancer element required for 3.9 kb^{peri} expression in the PNS and distal OFT cardiac cushions and that this sequence contains binding sites for YY1, implicating it as a regulator of *periostin* expression in the Schwann cell and cardiac OFT endocardial cushion cell lineages.

Discussion

Periostin is normally expressed in a wide spectrum of embryonic and adult mouse tissues (Kruzynska-Frejtag et al., 2001; Lindsley et al., 2005) and yet our results demonstrate the *cis*-elements which control the vast majority of endogenous periostin expression do not reside within the immediate 5′ upstream 3.9 kb^{peri} sequence. Instead, we found only a subset of *periostin* expression domains are regulated by this ~4 kb proximal region, suggesting the existence of additional undiscovered regulatory elements elsewhere. Bioinformatic analysis supports this contention by revealing several additional peaks of identity 3′ of 3.9 kb^{peri}, including intronic regions (data not shown). While these other homology peaks may harbor important regulatory elements, caution must be exercised in attempting to predict which regions are independently capable of driving transcription based solely on sequence identity.

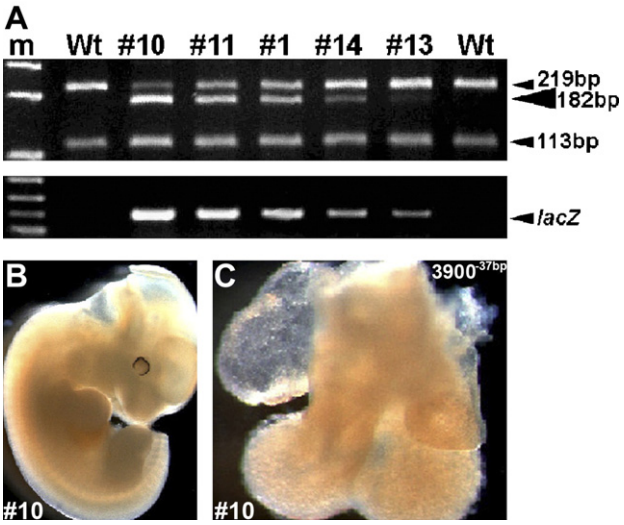

Fig. 9. Transgenic F_0 analysis of *periostin* 37-bp enhancer requirement. (A) PCR screening results of *Hsp68*-3900$^{-37\ bp}$ F_0 transient transgenic embryos that each contain the 3.9-kb^{peri} promoter minus the YY1-binding 37 bp fragment. Five embryos (#s10, 11, 1, 14, 13 placed in copy # order) were obtained, each of which carried the endogenous *periostin* promoter (identified as 113 and 219 bp PCR fragments following internal *Sac*II diagnostic digestion) as well as the *Hsp68*-3900$^{-37\ bp}$-containing transgenic promoter (identified as a separate 182 bp fragment, upper panel). Note that the intensity of the transgene (182 bp band) varies, while the endogenous bands are invariant. Although all five contained the *lacZ* transgene (verified via subsequent lacZ-specific PCR screening, lower panel), no β-galactosidase-positive cells could be detected (even after a weeks X-gal staining at 37 °C). Non-transgenic littermates were used as negative controls. (B and C) E12.5 whole embryo and isolated *Hsp68*-3900$^{-37\ bp}$ heart (#10 has highest transgene copy #) stained for *lacZ* reporter activity. Note the lack of *lacZ* reporter activity when the 37-bp internal enhancer is deleted within the context of the 3.9-kb^{peri} promoter (3900$^{-37\ bp}$; $n=5$). Thus, deletion of an internal 37 bp upstream region in the 3.9 kb^{peri} promoter completely abolishes *lacZ* reporter activity throughout the entire embryo.

Evaluation of transcriptional activity using cell-culture based functional assays can produce misleading data and requires verification by *in vivo* experimentation. Thus, generation of transgenic reporter mouse lines remains the gold standard for assessing the transcriptional activity of putative enhancer and/or repressor elements. Our dissection of 3.9 kb$^{peri\text{-}lacZ}$ stands as a case in point. For instance, our *in vitro* studies proved reliably predicative for isolating the Schwann cell enhancer module, but there was no reason to predict the co-capture of the OFT endocardial cushion enhancer. Similarly, Oshima et al. (2002) described a putative *Twist* site (E-box) located 468 bp upstream of the *periostin* transcription start that is capable of driving reporter expression *in vitro* in mouse MC3T3-E1 osteoblast cells. Interestingly, we also detect Twist-dependent transactivation in tissue culture when using various mouse mammary tumor cell lines (ABF and SJC, unpublished data). Despite the presence of this conserved E-box in our 3.9 kb$^{peri\text{-}lacZ}$ reporter mice, we were unable to detect *lacZ* expression in either the periosteum or cranial suture structures *in vivo*. While this identified *Twist* site may require additional up or downstream elements to function *in vivo*, the 3.9-kb$^{peri\text{-}lacZ}$ data suggest that it is unlikely to be involved in *in vivo* Schwann cell and distal OFT cushion regulation.

Even more striking is the finding of a regulatory element(s) within the 3.9-kb^{peri} that are active in both cardiac OFT and Schwann cells, two such seemingly disparate and highly specific cell populations. This raises questions about possible links between the transcriptional profiles of these two developmentally distinct cell types. Interestingly, Schwann cells and truncal OFT mesenchymal cardiac cushion cells both derive from neural crest cell precursors that have undergone EMT and have migrated to new anatomical locations and express YY1. Significantly, both *YY1* and *periostin* are both amongst a group of 100 genes identified as being upregulated in the solid tumors (Pilarsky et al., 2004). Given *periostin*'s upregulation in numerous neoplasias and its association with tumor metastasis, transcriptional activation of *periostin* via the identified PNS/cardiac-OFT enhancer could be driven by transcription factors that promote cell motility or migration. This idea is consistent with *periostin*'s suggested function as a homophilic adhesion molecule and marker of post-EMT mesenchymal maturation.

Schwann cells and cardiac cushion mesenchyme are also linked by their dependence on the neuregulin-ErbB signaling pathway. Targeted deletions of *neuregulin-1* (*glial growth factor*), *ErbB2* and *ErbB3* all result in early embryonic lethality secondary to cardiac malformation while also ablating the vast majority of developing Schwann cells (Erickson et al., 1997; Camenisch et al., 2002). Schwann cells and cardiac cushion mesenchyme also occupy tissue niches with similar ECM compositions. Hyaluronan, a major component of the cardiac cushion and myelin sheath ECM, is capable of activating ErbB3 in AV canal explants. Furthermore, AV explants from *hyaluronan synthase-2* (*Has2*) knockout mice, which typically fail to form cushion mesenchyme, are rescued by the pharmacological activation of ErbB2 and ErbB3 (Eggli et al., 1992; Spicer et al., 2002). Unfortunately, Has2 knockout embryos die too early (E9.0) to assess if they suffer from Schwann cell developmental defects, but a proposed Has2-conditional knockout mouse (Spicer et al., 2002) has the potential to address the role of hyaluronan in Schwann cell development in the near future.

In addition, Schwann and endocardial cushion cells share a number of molecular markers. Just as Schwann cells express the EF-hand containing protein S-100, so too do cardiac fibroblast-like cells, which are densely distributed throughout the cardiac skeleton, within the four cardiac valves and in the cardiac chordae tendoneae (Masani et al., 1986). Similarly, Oki et al. (1995) demonstrated that several glial and Schwann cell markers in addition to *S-100* (*glial fibrillary acidic protein* and *neurofilament protein*) are distributed along the subendocardial site of developing cardiac valves. Finally, the Schwann cell marker *Sox10* (as well as *Sox 8* and *9*) is co-expressed at the sites of endogenous *periostin* localization within the developing heart valves and autonomic nerves of the embryonic heart (Montero et al., 2002). The fact that Schwann cells and endocardial cushion cells express similar combinations of proteins, including transcription factors, suggests that their transcriptional programs overlap, even if their ultimate phenotypes diverge.

Advances in our understanding of eukaryotic gene transcription have illuminated how combinations of

transcription factors act in concert to *trans*-activate or *trans*-repress gene expression and help to explain how 'ubiquitous' transcription factors can modulate lineage/tissue-specific gene programs (Novina and Roy, 1996; Veitia, 2003). Existing as an enigmatic lynchpin, YY1 is known to be both a transcriptional repressor and/or activator and has been show to physically interact with more than a dozen proteins; including p300, CREB, Hdac2, E1A, FKBP25, C/EBP, c-myc, B23 and Stat5 (Shia et al., 1997; Bergad et al., 2000; Inouye and Seto, 1994; Shrivastava and Calame, 1994) that may cooperatively result in tissue restricted transcriptional regulation. YY1 is essential for embryonic life with its loss leading to peri-implantation lethality (Donohoe et al., 1999). Hundreds of genes may be directly and indirectly regulated by YY1, although the exact mechanism through which the factor acts remains unclear in many cases (Inouye and Seto, 1994; Donohoe et al., 1999). Recent data suggested that YY1 might induce chromatin remodeling in target genes through the recruitment of histone-modifying enzymes (Thomas and Seto, 1999). Furthermore, the manipulation of YY1 gene dosage has also been shown to profoundly alter global gene expression in the developing embryo (Affar et al., 2006). With specific regard to the developing cardiac valves, supportive data are starting to emerge that show SMAD-mediated modulation of YY1 activity can regulate BMP responses and cardiac-specific expression of a GATA4/5/6-dependent *Nkx2.5* enhancer (Lee et al., 2004). Thus, YY1 could be acting as a novel SMAD-interacting protein that represses SMAD transcriptional activities in a gene-specific manner and therefore regulates cell differentiation induced by TGFβ superfamily pathways (Kurisaki et al., 2003).

This study has defined a novel Schwann cell and distal OFT cushion-specific enhancer that links the transcriptional programs of these two divergent lineages and has improved our understanding of the likely upstream mechanisms that regulate expression. Understanding how *periostin*'s spatio-temporal expression pattern is driven is the first step to facilitating the development of experimental tools essential for studying the role of *periostin* in pathological disorders such as neuromas, nerve tumors and cardiac valve malformations. Additionally, the 3.9-kb^{peri} promoter can be utilized to drive tissue-specific expression of *Cre recombinase* in transgenic mice, and given the current lack of any cardiac endocardial cushion-restricted promoters (never mind one that will enable the molecular characterization of inlet verses outflow cushion morphogenesis) this may be a useful molecular reagent. Our analysis has provided potential links between precursor Schwann cells and OFT endocardial cushion lineages and also implicated the YY1 protein in post-migratory neural crest differentiation events. Finally, uncovering the additional *trans*-factors and *cis*-elements that regulate *periostin*'s expression in these and other tissues is the subject of ongoing investigations, the results of which will provide greater insights into the mechanisms by which the tissues of the developing mammalian embryo so precisely determine their cell identity and fate.

Acknowledgments

Special thanks to Drs. Joe Bidwell and Simon Rhodes for their helpful advice. These studies were supported, in part, by an American Heart Association Midwest Predoctoral Fellowship to AL, National Institutes of Health Training in Vascular Biology and Medicine T32 HL079995 postdoctoral support for PS, Riley Children's Foundation support for HZ and HL60714 grant and IU Department of Pediatrics/Cardiology support for SJC.

References

Affar, E.B., Gay, F., Shi, Y., Liu, H., Huarte, M., Wu, S., Collins, T., Li, E., Shi, Y., 2006. Essential dosage-dependent functions of the transcription factor yin yang 1 in late embryonic development and cell cycle progression. Mol. Cell. Biol. 26, 3565–3581.

Bao, S., Ouyang, G., Bai, X., Huang, Z., Ma, C., Liu, M., Shao, R., Anderson, R., Rich, J., Wang, X., 2004. Periostin potently promotes metastatic growth of colon cancer by augmenting cell survival via the Akt/PKB pathway. Cancer Cell 5, 329–339.

Bergad, P.L., Towle, H.C., Berry, S.A., 2000. Yin-yang 1 and glucocorticoid receptor participate in the stat5-mediated growth hormone response of the serine protease inhibitor 2.1 gene. J. Biol. Chem. 275, 8114–8120.

Britsch, S., Goerich, D.E., Riethmacher, D., Peirano, R.I., Rossner, M., Nave, K.-A., Birchmeier, C., Wegner, M., 2001. The transcription factor Sox10 is a key regulator of peripheral glial development. Genes Dev. 15, 66–78.

Camenisch, T.D., Schroeder, J.A., Bradley, J., Klewer, S.E., McDonald, J.A., 2002. Heart-valve mesenchyme formation is dependent on hyaluronan-augmented activation of ErbB2-ErbB3 receptors. Nat. Med. 8, 850–855.

Conway, S.J., Bundy, J., Chen, J., Dickman, E., Rogers, R., Will, B.M., 2000. Abnormal neural crest stem cell expansion is responsible for the conotruncal heart defects within the Splotch (Sp^{2H}) mouse mutant. Cardiovasc. Res. 47, 314–328.

Conway, S.J, Kruzynska-Frejtag, A., Kneer, P.L., Machnicki, M., Koushik, S.V., 2003. What cardiovascular defect does my prenatal mouse mutant have, and why? Genesis 35, 1–21.

Dignam, J., Martin, P., Shastry, B., Roeder, R., 1983. Eukaryotic gene transcription with purified components. Methods Enzymol. 101, 582–598.

Donohoe, M.E., Zhang, X., McGinnis, L., Biggers, J., Li, E., Shi, Y., 1999. Targeted disruption of mouse Yin Yang 1 transcription factor results in peri-implantation lethality. Mol. Cell. Biol. 19, 7237–7244.

Eggli, P.S., Lucocq, J., Ott, P., Graber, W., Zypen, E.v.d., 1992. Ultrastructural localization of hyaluronan in myelin sheaths of the rat central and rat and human peripheral nervous systems using hyaluronan-binding protein-gold and link protein-gold. Neuroscience 48, 737–744.

Erickson, S.L., O'Shea, K.S., Ghaboosi, N., Loverro, L., Frantz, G., Bauer, M., Lu, L.H., Moore, M.W., 1997. ErbB3 is required for normal cerebellar and cardiac development: a comparison with ErbB2-and heregulin-deficient mice. Development 124, 4999–5011.

Firulli, A.B., Olson, E., 1997. Modular regulation of muscle gene transcription: a mechanism for muscle cell diversity. Trends Genet. 13, 364–369.

Flanagan, J.R., Becker, K.G., Ennist, D.L., Gleason, S.L., Driggers, P.H., Levi, B.Z., Appella, E., Ozato, K., 1992. Cloning of a negative transcription factor that binds to the upstream conserved region of Moloney murine leukemia virus. MCB 12, 38–44.

Gillan, L., Matei, D., Fishman, D.A., Gerbin, C.S., Karlan, B.Y., Chang, D.D., 2002. Periostin secreted by epithelial ovarian carcinoma is a ligand for {alpha}V{beta}3 and {alpha}V{beta}5 integrins and promotes cell motility. Cancer Res. 62, 5358–5364.

Gonzalez, H., Gujrati, M., Frederick, M., Henderson, Y., Arumugam, J., Spring, P., Mitsudo, K., Kim, H., Clayman, G., 2003. Identification of 9 genes differentially expressed in head and neck squamous cell carcinoma. Arch. Otolaryngol., Head Neck Surg. 129, 754–759.

Gonzalez-Martinez, T., Perez-Piñera, P., Díaz-Esnal, B., Vega, J.A., 2003. S-100 proteins in the human peripheral nervous system. Microsc. Res. Tech. 60, 633–638.

Gordon, S., Akopyan, G., Garban, H., Bonavida, B., 2005. Transcription factor YY1: structure, function, and therapeutic implications in cancer biology. Oncogene 25, 1125–1142.

Gronroos, E., Terentiev, A.A., Punga, T., Ericsson, J., 2004. YY1 inhibits the activation of the p53 tumor suppressor in response to genotoxic stress. Proc. Natl. Acad. Sci. 101, 12165–12170.

Hai, M., Muja, N., DeVries, G.H., Quarles, R.H., Patel, P.I., 2002. Comparative analysis of Schwann cell lines as model systems for myelin gene transcription studies. J. Neurosci. Res. 69, 497–508.

Horiuchi, K., Amizuka, N., Takeshita, S., Takamatsu, H., Katsuura, M., Ozawa, H., Toyama, Y., Bonewald, L., Kudo, A., 1999. Identification and characterization of a novel protein, periostin, with restricted expression to periosteum and periodontal ligament and increased expression by transforming growth factor beta. J. Bone Miner. Res. 14, 1239–1249.

Inouye, C.J., Seto, E., 1994. Relief of YY1-induced transcriptional repression by protein-protein interaction with the nucleolar phosphoprotein B23. J. Biol. Chem. 269, 6506–6510.

Jessen, K.R., Mirsky, R., 2002. Signals that determine Schwann cell identity. J. Anat. 200, 367–376.

Jessen, K.R., Mirsky, R., 2005. The origin and development of glial cells in peripheral nerves. Nat. Rev., Neurosci. 6, 671–682.

Jiang, X., Rowitch, D.H., Soriano, P., McMahon, A.P., Sucov, H.M., 2000. Fate of the mammalian cardiac neural crest. Development 127, 1607–1616.

Kawamoto, T., Noshiro, M., Shen, M., Nakamasu, K., Hashimoto, K., Kawashima-Ohya, Y., Gotoh, O., Kato, Y., 1998. Structural and phylogenetic analyses of RGD-CAP/[beta]ig-h3, a fasciclin-like adhesion protein expressed in chick chondrocytes. Biochim. Biophys. Acta (BBA)—Gene Struct. Expr. 1395, 288–292.

Kii, I., Amizuka, N., Minqi, L., Kitajima, S., Saga, Y., Kudo, A., 2006. Periostin is an extracellular matrix protein required for eruption of incisors in mice. Biochem. Biophys. Res. Commun. 342, 766–772.

Kothary, R., Clapoff, S., Darling, S., Perry, M., Moran, L., Rossant, J., 1989. Inducible expression of an hsp68-lacZ hybrid gene in transgenic mice. Development 105, 707–714.

Kruzynska-Frejtag, A., Machnicki, M., Rogers, R., Markwald, R., Conway, S.J., 2001. Periostin (an osteoblast-specific factor) is expressed within the embryonic mouse heart during valve formation. Mech. Dev. 103, 183–188.

Kruzynska-Frejtag, A., Wang, J., Maeda, M., Rogers, R., Krug, E., Hoffman, S., Markwald, R.R., Conway, S.J., 2004. Periostin is expressed within the developing teeth at the sites of epithelial–mesenchymal interaction. Dev. Dyn. 229, 857–868.

Kudo, Y., Ogawa, I., Kitajima, S., Kitagawa, M., Kawai, H., Gaffney, P.M., Miyauchi, M., Takata, T., 2006. Periostin promotes invasion and anchorage-independent growth in the metastatic process of head and neck cancer. Cancer Res. 66, 6928–6935.

Kuhlbrodt, K., Herbarth, B., Sock, E., Hermans-Borgmeyer, I., Wegner, M., 1998. Sox10, a novel transcriptional modulator in glial cells. J. Neurosci. 18, 237–250.

Kurisaki, K., Kurisaki, A., Valcourt, U., Terentiev, A.A., Pardali, K., ten Dijke, P., Heldin, C.-H., Ericsson, J., Moustakas, A., 2003. Nuclear factor YY1 inhibits transforming growth factor {beta}-and bone morphogenetic protein-induced cell differentiation. Mol. Cell. Biol. 23, 4494–4510.

Le Douarin, N.M., Dulac, C., Dupin, E., Cameron-Curry, P., 1991. Glial cell lineages in the neural crest. Glia 4, 175–184.

Lee, T.C., Shi, Y., Schwartz, R.J., 1992. Displacement of BrdUrd-induced YY1 by serum response factor activates skeletal alpha-actin transcription in embryonic myoblasts. Proc. Natl. Acad. Sci. 89, 9814–9818.

Lee, K.-H., Evans, S., Ruan, T.Y., Lassar, A.B., 2004. SMAD-mediated modulation of YY1 activity regulates the BMP response and cardiac-specific expression of a GATA4/5/6-dependent chick Nkx2.5 enhancer. Development 131, 4709–4723.

Li, G., Oparil, S., Sanders, J., Zhang, L., Dai, M., Chen, L., Conway, S., McNamara, C., Sarembock, I., 2005. Phosphatidylinositol-3-kinase signaling mediates vascular smooth muscle cell expression of periostin in vivo and in vitro. Atherosclerosis 188, 292–300.

Lindsley, A., Li, W., Wang, J., Maeda, N., Rogers, R., Conway, S.J., 2005. Comparison of the four mouse fasciclin-containing genes expression patterns during valvuloseptal morphogenesis. Gene Expr. Patt. 5, 593–600.

Litvin, J., Selim, A.-H., Montgomery, M.O., Lehmann, K., Rico, M.C., Devlin, H., Bednarik, D.P., Safadi, F.F., 2004. Expression and function of periostin-isoforms in bone. J. Cell. Biochem. 92, 1044–1061.

Litvin, J., Zhu, S., Norris, R., Markwald, R., 2005. Periostin family of proteins: therapeutic targets for heart disease. Anat. Rec. Part A: Discoveries Mol. Cell. Evol. Biol. 287A, 1205–1212.

Loots, G.G., Ovcharenko, I., 2004. rVISTA 2.0: evolutionary analysis of transcription factor binding sites. Nucleic Acids Res. 32, W217–W221.

Madison, D., Kruger, W., Kim, T., Pfeiffer, S., 1996. Differential expression of rab3 isoforms in oligodendrocytes and astrocytes. J. Neurosci. Res. 45, 258–268.

Masani, F., Iwanaga, T., Shibata, A., Fujita, T., 1986. Immunohistochemical demonstration of S-100 protein in fibroblast-like cells of the guinea-pig heart. Arch. Histol. Jpn. 49, 117–127.

McAllister, L., Goodman, C., Zinn, K., 1992. Dynamic expression of the cell adhesion molecule fasciclin I during embryonic development in Drosophila. Development 115, 267–276.

McFadden, D.G., Charite, J., Richardson, J.A., Srivastava, D., Firulli, A.B., Olson, E.N., 2000. A GATA-dependent right ventricular enhancer controls dHAND transcription in the developing heart. Development 127, 5331–5341.

Miskimins, R., Miskimins, W., 2001. A role for an AP-1-like site in the expression of the myelin basic protein gene during differentiation. Int. J. Dev. Neurosci. 19, 85–91.

Montero, J., Giron, B., Arrechedera, H., Cheng, Y., Scotting, P., Chimal-Monroy, J., Garcia-Porrero, J., Hurle, J., 2002. Expression of Sox8, Sox9 and Sox10 in the developing valves and autonomic nerves of the embryonic heart. Mech. Dev. 118, 199–202.

Norris, R., Damon, B., Mironov, V., Kasyanov, V., Ramamurthi, A., Moreno-Rodriguez, R., Trusk, T., Potts, J.D., Goodwin, R.L., Davis, J., Hoffman, S., Wen, X., Sugi, Y., Kern, C.B., Mjaatvedt, C.H., Turner, D.K., Oka, T., Conway, S.J., Molkentin, J.D., Forgacs, G., Markwald, R.R., 2007. Periostin regulates collagen fibrillogenesis and the biomechanical properties of connective tissues. J. Cell. Biochem. 101 (3), 695–711.

Novina, C., Roy, A., 1996. Core promoters and transcriptional control. Trends Genet. 12, 351–355.

Oki, T., Fukuda, N., Kawano, T., Iuchi, A., Tabata, T., Manabe, K., Kageji, Y., Sasaki, M., Yamada, H., Ito, S., 1995. Histopathologic studies of innervation of normal and prolapsed human mitral valves. J. Heart Valve Dis. 4, 496–502.

Oshima, A., Tanabe, H., Yan, T., Lowe, G., Glackin, C., Kudo, A., 2002. A novel mechanism for the regulation of osteoblast differentiation: transcription of periostin, a member of the fasciclin I family, is regulated by the bHLH transcription factor, twist. J. Cell. Biochem. 86, 792–804.

Ovcharenko, I., Loots, G.G., Hardison, R.C., Miller, W., Stubbs, L., 2004. zPicture: dynamic alignment and visualization tool for analyzing conservation profiles. Genome Res. 14, 472–477.

Pilarsky, C., Wenzig, M., Specht, T., Saeger, H.D., Grutzmann, R., 2004. Identification and validation of commonly overexpressed genes in solid tumors by comparison of microarray data. Neoplasia 6, 744–750.

Rios, H., Koushik, S.V., Wang, H., Wang, J., Zhou, H.-M., Lindsley, A., Rogers, R., Chen, Z., Maeda, M., Kruzynska-Frejtag, A., Feng, J.Q., Conway, S.J., 2005. periostin null mice exhibit dwarfism, incisor enamel defects, and an early-onset periodontal disease-like phenotype. Mol. Cell. Biol. 25, 11131–11144.

Sasaki, H., Sato, Y., Kondo, S., Fukai, I., Kiriyama, M., Yamakawa, Y., Fuji, Y., 2002. Expression of the periostin mRNA level in neuroblastoma. J. Pediatr. Surg. 37, 1293–1297.

Sasaki, H., Yu, C.-Y., Meiru Dai, C.T., Loda, M., Auclair, D., Chen, L.B., Elias, A., 2004. Elevated serum periostin levels in patients with bone metastases from breast but not lung cancer. Breast Cancer Res. Treat. 77, 245–252.

Shia, Y., Leeb, J.-S., Galvin, K.M., 1997. Everything you have ever wanted to know about Yin Yang 1. Biochim. Biophys. Acta (BBA)—Rev. Cancer 1332, F49–F66.

Shrivastava, A., Calame, K., 1994. An analysis of genes regulated by the multi-functional transcriptional regulator Yin Yang-1. Nucleic Acid Res. 22, 5151–5155.

Spicer, A.P., Tien, J.L., Joo, A., Bowling Jr., R.A.B., 2002. Investigation of hyaluronan function in the mouse through targeted mutagenesis. Glycoconj. J. 19, 341–345.

Stanton, L.W., Garrard, L.J., Damm, D., Garrick, B.L., Lam, A., Kapoun, A.M., Zheng, Q., Protter, A.A., Schreiner, G.F., White, R.T., 2000. Altered patterns of gene expression in response to myocardial infarction. Circ. Res. 86, 939–945.

Sun, Y., Liang, X., Najafi, N., Cass, M., Lin, L., Cai, C., Chen, J., Evans, S., 2007. Islet 1 is expressed in distinct cardiovascular lineages, including pacemaker and coronary vascular cells. Dev. Biol. 304 (1), 286–296 (Apr 1).

Takayama, G., Arima, K., Kanaji, T., Toda, S., Tanaka, H., Shoji, S., McKenzie, A., Nagai, H., Hotokebuchi, T., Izuhara, K., 2006. Periostin: a novel component of subepithelial fibrosis of bronchial asthma downstream of IL-4 and IL-13 signals. J. Allergy Clin. Immunol. 118, 98–104.

Takeshita, S., Kikuno, R., Tezuka, K., Amann, E., 1993. Osteoblast-specific factor 2: cloning of a putative bone adhesion protein with homology with the insect protein fasciclin I. Biochem. J. 294, 271–278.

Thomas, M., Seto, E., 1999. Unlocking the mechanisms of transcription factor YY1: are chromatin modifying enzymes the key? Gene 236, 197–208.

Thompson, J., Higgins, D., Gibson, T., 1994. CLUSTAL W: improving the sensitivity of progressive multiple sequence alignment through sequence weighting, position-specific gap penalties and weight matrix choice. Nucleic Acid Res. 22, 4673–4680.

Toda, K., Small, J.A., Goda, S., Quarles, R.H., 1994. Biochemical and cellular properties of three immortalized Schwann cell lines expressing different levels of the myelin-associated glycoprotein. J. Neurochem. 63, 1646–1657.

Veitia, R., 2003. A sigmoidal transcriptional response: cooperativity, synergy and dosage effects. Biol. Rev. Camb. Philos. Soc. 78, 149–170.

Wang, C.-C., Chen, J.J.W., Yang, P.-C., 2006. Multifunctional transcription factor YY1: a therapeutic target in human cancer? Expert Opin. Ther. Targets 10, 253–266.

Wegner, M., 2000. Transcriptional control in myelinating glia: flavors and spices. Glia 31, 1–14.

Yang, J., Mani, S.A., Donaher, J.L., Ramaswamy, S., Itzykson, R.A., Come, C., Savagner, P., Gitelman, I., Richardson, A., Weinberg, R.A., 2004. Twist, a master regulator of morphogenesis, plays an essential role in tumor metastasis. Cell 117, 927–939.

Yarden, Y., Sliwkowski, M., 2001. Untangling the ErbB signalling network. Nat. Rev., Mol. Cell. Biol. 2, 127–137.

Ye, J., Young, H.A., Ortaldo, J.R., Ghosh, P., 1994. Identification of a DNA binding site for the nuclear factor YY1 in the human GM-CSF core promoter. Nucleic Acid Res. 22, 5672–5678.

Ye, J., Cippitelli, M., Dorman, L., Ortaldo, J.R., Young, H.A., 1996. The nuclear factor YY1 suppresses the human gamma interferon promoter through two mechanisms: inhibition of AP1 binding and activation of a silencer element. MCB 16, 4744–4753.